

# Revisiting the Polyoxometalate-Based Late-Transition-Metal-Oxo Complexes: The “Oxo Wall” Stands

Kevin P. O'Halloran,<sup>†</sup> Chongchao Zhao,<sup>†</sup> Nicole S. Ando,<sup>†</sup> Arthur J. Schultz,<sup>‡</sup> Thomas F. Koetzle,<sup>‡</sup> Paula M. B. Piccoli,<sup>‡</sup> Britt Hedman,<sup>§</sup> Keith O. Hodgson,<sup>§</sup> Elena Bobyr,<sup>§</sup> Martin L. Kirk,<sup>||</sup> Sushilla Knottenbelt,<sup>||</sup> Ezra C. Depperman,<sup>||</sup> Benjamin Stein,<sup>||</sup> Travis M. Anderson,<sup>†</sup> Rui Cao,<sup>†</sup> Yurii V. Geletii,<sup>†</sup> Kenneth I. Hardcastle,<sup>†</sup> Djamaladdin G. Musaev,<sup>⊥</sup> Wade A. Neiwert,<sup>†</sup> Xikui Fang,<sup>†</sup> Keiji Morokuma,<sup>†,⊥</sup> Shaoxiong Wu,<sup>†</sup> Paul Kögerler,<sup>#,○</sup> and Craig L. Hill<sup>\*,†</sup>

<sup>†</sup>Department of Chemistry, Emory University, Atlanta, Georgia 30322, United States

<sup>‡</sup>Intense Pulsed Neutron Source, Argonne National Laboratory, Argonne, Illinois 60439, United States

<sup>§</sup>Department of Chemistry and Stanford Synchrotron Radiation Lightsource, SLAC, Stanford University, Stanford, California 94305, United States

<sup>||</sup>Department of Chemistry and Chemical Biology, The University of New Mexico, Albuquerque, New Mexico 87131-0001, United States

<sup>⊥</sup>Cherry L. Emerson Center for Scientific Computation, Emory University, Atlanta, Georgia 30322, United States

<sup>#</sup>Ames Laboratory, Iowa State University, Ames, Iowa 50011, United States

## Supporting Information

**ABSTRACT:** Terminal oxo complexes of the late transition metals Pt, Pd, and Au have been reported by us in *Science* and *Journal of the American Chemical Society*. Despite thoroughness in characterizing these complexes (multiple independent structural methods and up to 17 analytical methods in one case), we have continued to study these structures. Initial work on these systems was motivated by structural data from X-ray crystallography and neutron diffraction and <sup>17</sup>O and <sup>31</sup>P NMR signatures which all indicated differences from all previously published compounds. With significant new data, we now revisit these studies. New X-ray crystal structures of previously reported complexes  $K_{14}[P_2W_{19}O_{69}(OH_2)]$  and  $K_{10}Na_3[Pd^{IV}(O)(OH)WO(OH_2)(PW_9O_{34})_2]$  and a closer examination of these structures are provided. Also presented are the <sup>17</sup>O NMR spectrum of an <sup>17</sup>O-enriched sample of  $[PW_{11}O_{39}]^{7-}$  and a careful combined <sup>31</sup>P NMR-titration study of the previously reported  $K_7H_2[Au(O)(OH_2)P_2W_{20}O_{70}(OH_2)_2]$ . These and considerable other data collectively indicate that previously assigned terminal Pt-oxo and Au-oxo complexes are in fact cocrystals of the all-tungsten structural analogues with noble metal cations, while the Pd-oxo complex is a disordered Pd(II)-substituted polyoxometalate. The neutron diffraction data have been re-analyzed, and new refinements are fully consistent with the all-tungsten formulations of the Pt-oxo and Au-oxo polyoxometalate species.

Sc	Ti	V	Cr	Mn	Fe	Co	Ni	Cu	Zn
Y	Zr	Nb	Mo	Tc	Ru	Rh	Pd	Ag	Cd
La	Hf	Ta	W	Re	Os	Ir	Pt	Au	Hg

## INTRODUCTION

Many of the catalysts and O<sub>2</sub>-based technologies that are of global importance are based on the late-transition-metal elements. Terminally bound oxo species of these metals are proposed to be key intermediates in these important and useful reactions.<sup>1</sup> A terminal oxo ligand is a doubly or triply bonded oxygen atom which acts as a multielectron donor to one electrophilic transition metal. Despite over 40 years of effort from the research community to isolate such complexes of the late transition elements, they still remain elusive. The scarcity of these compounds is due to electronic repulsion between oxo ligands (or other multiply bonded ligands) and high d-count transition metals in tetragonal environments and was explained by molecular orbital calculations,<sup>2</sup> supported experimentally,<sup>3</sup> and later extended to other geometries by Mayer et al.<sup>4</sup> Holm has reviewed a large number of metal oxo complexes and concludes that “M=O groups are stabilized at metal centers

with an oxidation state of no less than 4+ and no more than four d electrons.”<sup>5</sup> Consequently, oxo complexes of the early transition elements (groups 3–6) are extremely stable and abundant. Those of the midtransition elements (groups 7–8) are generally more reactive and intensely investigated, and those of the late transition elements (groups 9–11) are rarely reported. This combination of theory and observations has given rise to the defensible concept of the “Oxo Wall”, in particular articulated by Gray and Winkler: transition metals to the right of the Fe–Ru–Os group will not support a terminal oxo ligand in a tetragonal environment,<sup>6</sup> since d electrons here begin to populate orbitals that are antibonding in the M=O unit.<sup>7</sup> There are a handful of interesting examples that are exceptions to these guidelines:  $[Fe^{III}H_3L(O)]^{2-}$  where L =

Received: April 28, 2011

Published: June 13, 2012



tris[(*N'*-*tert*-butylureaylato)-*N*-ethyl]aminato and  $[\text{Re}^{\text{III}}(\text{O})\text{I}(\text{RCCR}')_2]$  are terminal oxo complexes with oxidation states of less than +4.<sup>4,8</sup> The complexes  $[\text{Ir}(\text{O})(2,4,6\text{-trimethylphenyl})_3]$  and  $[\text{Pt}(\text{O})\text{-PCN}]^+$  where  $\text{PCN} = \text{C}_6\text{H}_3[\text{CH}_2\text{P}(\text{tBu})_2](\text{CH}_2)_2\text{N}(\text{CH}_3)_2$  are terminal oxo complexes of elements to the right of the Fe–Ru–Os group but do not violate the Oxo Wall because they are not of tetragonal geometry.<sup>6a,9,10</sup> These four examples push the limits of terminal metal-oxo chemistry, but the Oxo Wall holds true for all transition metal complexes in tetragonal environments.

Polyoxometalates (POMs) are early transition metal oxide clusters that exhibit a wide range of reactivity and bonding to many different elements. In particular, polyoxometalates have previously been shown to effectively coordinate several of the late transition metals, and this area has just been reviewed.<sup>11</sup> In addition, polyoxometalates have long been known to have  $\pi$ -accepting character when present as ligands.<sup>12</sup> We therefore endeavored to use POMs to coordinate and stabilize the highly sought metal-oxo species. We reported late-transition-metal-oxo complexes of Pt,<sup>13</sup> Pd,<sup>14</sup> and Au<sup>15</sup> elements based on multiple independent lines of evidence derived from 10, 15, and 17 experimental techniques, respectively (see Supporting Information, SI, for complete list), and we included multiple established experts in diffraction and other structural methods as collaborators and coauthors. The merits of these complexes have been discussed by us and others recently.<sup>16,17</sup> Ulrich Kortz of Jacobs University (Bremen, Germany) made some observations on our systems and suggested that the data in our original publications did not necessarily prove the existence of terminal oxo species in these complexes. New data from our laboratory now establish the correct assignments. Herein, we report new X-ray crystal structures of the previously published<sup>18</sup>  $\text{K}_{14}[\text{P}_2\text{W}_{19}\text{O}_{69}(\text{OH}_2)]$  (1), the <sup>17</sup>O NMR spectrum of  $(\text{CH}_3(\text{CH}_2)_3)_4\text{N}_7[\text{PW}_{11}\text{O}_{39}]$  (2), a careful titration of “ $\text{K}_7\text{H}_2[\text{Au}(\text{O})(\text{OH}_2)\text{P}_2\text{W}_{20}\text{O}_{70}(\text{OH}_2)_2]$ ” followed by <sup>31</sup>P NMR spectroscopy, and a new X-ray crystal structure of the compound reformulated as  $\text{K}_{12}[\text{PdWO}(\text{OH}_2)(\text{PW}_9\text{O}_{34})_2]$  (3). On the basis of these new findings, we reanalyze the main conclusions in our previous seven-team studies and delineate the errors in our initial assessments.

## RESULTS AND DISCUSSION

The thermal ellipsoid plot of  $\text{K}_{14}[\text{P}_2\text{W}_{19}\text{O}_{69}(\text{OH}_2)]$  (1),  $\{\text{P}_2\text{W}_{19}\}$ , from data collected at 173 K is shown in Figure 1. The synthesis and room temperature X-ray crystal structure of this compound were originally reported by Tourné and Tourné in 1988.<sup>18</sup> The polyanion of 1 matches the originally reported structure except that the W10–O36 bond distance (1.737(17) Å) is substantially longer than the original structure (1.67 Å). The difference is due to the libration artifact in X-ray structures: terminally bound atoms, especially light atoms bound to heavy atoms, have an oscillatory motion perpendicular to the direction of the bond between the two atoms.

When the light atom is refined as a sphere or a spheroid, this movement can give an incorrectly short bond distance between the two atoms. At higher temperatures, libration and the resulting apparent bond distance “shortening” are more pronounced. Libration effects have been discussed<sup>19</sup> but are rarely reported in polyoxometalate crystallography.

In 2004, we reported a POM that was incorrectly formulated as the first Pt-oxo complex, “ $\text{K}_7\text{Na}_9[\text{Pt}^{\text{IV}}(\text{O})(\text{H}_2\text{O})(\text{PW}_9\text{O}_{34})_2]$ .”<sup>13</sup> Quotes here denote our original incorrect formulation. A summary of the original and our new

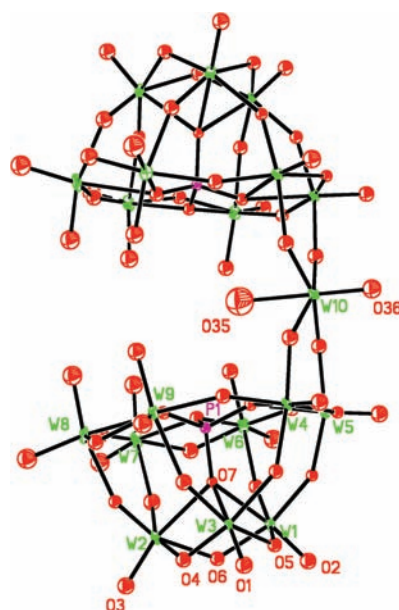


**Figure 1.** Thermal ellipsoid plot of  $[\text{P}_2\text{W}_{19}\text{O}_{69}(\text{OH}_2)]^{14-}$  (50% probability surfaces). Tungsten and phosphorus atoms are refined anisotropically; oxygens are refined isotropically.

(corrected) assignments is given in Table 1. In that study, we obtained the X-ray structure of brown crystals of this complex

**Table 1. Correct Formulations of Compounds**

original assignment	reference	new assignment
“ $\text{K}_7\text{Na}_9[\text{Pt}^{\text{IV}}(\text{O})(\text{H}_2\text{O})(\text{PW}_9\text{O}_{34})_2]$ ”	13	$\text{K}_{14}[\text{P}_2\text{W}_{19}\text{O}_{69}(\text{OH}_2)]$ (1)
“ $\text{K}_{15}\text{H}_2[\text{Au}(\text{O})(\text{OH}_2)\text{P}_2\text{W}_{18}\text{O}_{68}]$ ”	15	$\text{K}_{14}[\text{P}_2\text{W}_{19}\text{O}_{69}(\text{OH}_2)]$ (1)
“ $\text{K}_7\text{H}_2[\text{Au}(\text{O})(\text{OH}_2)\text{P}_2\text{W}_{20}\text{O}_{70}(\text{OH}_2)_2]$ ”	15	$\text{K}_4\text{H}_2[\text{P}_2\text{W}_{21}\text{O}_{71}(\text{OH}_2)_3]$
“ $\text{K}_{10}\text{Na}_3[\text{Pd}^{\text{IV}}(\text{O})(\text{OH})\text{WO}(\text{OH}_2)(\text{PW}_9\text{O}_{34})_2]$ ”	14	$\text{K}_{12}[\text{PdWO}(\text{OH}_2)(\text{PW}_9\text{O}_{34})_2]$ (3)

at 193 K and obtained a Pt=O distance of 1.720(18) Å, which was compared to the considerably shorter literature  $\text{W}\equiv\text{O}$  distance in  $\{\text{P}_2\text{W}_{19}\}$  of 1.67 Å. This difference was accepted as outside the possible range of error by the several crystallographic coauthors of our publications. The apparent novelty of a terminal Pt-oxo complex prompted us to do many additional confirmatory studies. One of these was a single-crystal neutron diffraction crystal structure showing no evidence of hydrogen atoms around the terminal oxo atom, ruling out a better preceded Pt–OH or Pt–OH<sub>2</sub> species established by 50 structures in the Cambridge Structural Database. We therefore concluded, along with considerable other evidence, that we had the assigned complex. However, when compared to the structure of 1 at 173 K, the corresponding terminal M–O bond distance in “ $\text{K}_7\text{Na}_9[\text{Pt}^{\text{IV}}(\text{O})(\text{H}_2\text{O})(\text{PW}_9\text{O}_{34})_2]$ ” is the same within experimental error. A close examination of the X-ray lattice parameters and a comparison of all of the characterization data reveal that our reported “ $\text{K}_7\text{Na}_9[\text{Pt}^{\text{IV}}(\text{O})(\text{H}_2\text{O})(\text{PW}_9\text{O}_{34})_2]$ ” is in fact  $\{\text{P}_2\text{W}_{19}\}$  with small amounts of cocrystallized Pt(II). In the original work, we conducted triplicate elemental analyses from three different analytical laboratories, consistent with the thoroughness of the work. However, repeated syntheses and elemental analyses show that variable amounts of Pt(II) counter cations can be incorporated into the crystals, although they were not located in the original crystal structure. This fact accounts for the brown color and

misleading elemental analysis results. Thus, we were originally misled by the seemingly unique M–O bond distance, the brown color of the crystals, and the structural information corroborated by neutron diffraction.

In an independent study in 2007, we incorrectly reported the first terminal Au-oxo complex, “ $K_{15}H_2[Au(O)(OH_2)P_2W_{18}O_{68}]$ ”, based on a similar manifold of complementary experimental arguments.<sup>15</sup> Given the potential for disorder in X-ray structures of polyoxometalates, we initially collected and reported three data sets at different temperatures on our putative Au-oxo (and Pd-oxo) complexes, which were found to be consistent with the original formulations. A neutron diffraction study showed no evidence of hydrogen atoms around the oxo atom and also indicated mixed occupancy of the central metal position as about two-thirds noble metal and one-third tungsten. Given the uniqueness of such a Au-oxo moiety, we sought even more confirmatory evidence in this case. This additional evidence was Au  $L_2$  edge X-ray absorption spectroscopy and both chemical and coulometric titrations, which all confirmed the presence of about one equivalent of Au(III) in bulk samples, and  $^{17}O$  NMR spectroscopy, which mistakenly noted the oxo bound to gold. These findings were supported by duplicate elemental analyses from three different analytical laboratories, and repeated syntheses of this complex lead to 1–1.5 equivalents of Au(III) per polyanion incorporated in the crystals. However, we now report that a comparison of the corresponding terminal M–O distance and lattice parameters in the X-ray crystal structures reveal that our reported “ $K_{15}H_2[Au(O)(OH_2)P_2W_{18}O_{68}]$ ” is in fact  $\{P_2W_{19}\}$  with an appreciable amount of cocrystallized Au(III) counter cations which are incorporated in the later stages of crystal growth. This occurs because POMs crystallize more rapidly with  $K^+$  ions in solution, but after initial crystal growth, the concentration of  $K^+$  decreases and Au(III) counter cations begin to compete with  $K^+$  ions for crystal incorporation. The Au(III) counter cations were not located in the original X-ray structures. Additionally, the X-ray absorption spectroscopy, cyclic voltammetry, coulometric studies, and all other original data are consistent with the new assignment presented here.

Reanalysis of the neutron structures is consistent with the new structural models, although not necessarily ruling out models with partial occupancies of W/Pt or W/Au. That is, substituting W with a fractional occupancy of unity for Pt or Au and refining just the W atom with the original single crystal neutron data gives an isotropic atomic displacement parameter (ADP) that is nearly equivalent to the other nine W atoms in the structure. While reanalyzing these structures, we also corrected a previously undetected error involving the metal-site multiplicity in the input model for the “Pt-oxo” structure that masked possible evidence for W on the Pt site. It should also be noted that varying the fractional occupancy with either W or Pt (or Au) is consistent with partial occupancy by both W and Pt or W and Au (as originally reported by us in the latter case), but with larger ADPs. Furthermore, re-examination of difference Fourier plots in the “Au-oxo” structure exhibits evidence for disorder of the Au or W atom about the special position. Refinement of this disordered model with two half-Au or two half-W atoms separated by 0.6 Å about a two-fold rotation axis gives reasonable results, although varying the occupancy with W is also consistent with partial Au occupancy. These structural models of mixed Au/W or Pt/W are ruled out by all of the other characterization data, which indicate that W and only W resides in that position. This result suggests that rather than

thermal motion of the oxygen atom, disorder of the metal atom may contribute to the short  $W\equiv O$  observed in the room temperature X-ray structure.<sup>18</sup>

Previously, we reported the  $^{17}O$  NMR of an  $^{17}O$ -enriched sample of “ $K_{15}H_2[Au(O)(OH_2)P_2W_{18}O_{68}]$ ” and observed, in addition to the  $W\equiv O$  and  $W-O-W$  peaks, an isolated peak at 580 ppm. A comparison to published  $^{17}O$  NMR chemical shift values of polytungstates and polymolybdates did not reveal any known peaks in this range, and thus we previously assigned this peak to the terminal Au-oxo oxygen. That assignment was made on the established correlation between chemical shift and oxygen  $\pi$ -bond order for tungsten oxo species as well as the experimentally determined diamagnetic nature of the complex.<sup>20</sup> At the time, we were unaware that “ $K_{15}H_2[Au(O)(OH_2)P_2W_{18}O_{68}]$ ” was actually  $\{P_2W_{19}\}$  and therefore did not consider the possible decomposition of  $\{P_2W_{19}\}$  to  $\{PW_{11}\}$ . The  $^{17}O$  NMR spectrum of this decomposition polytungstate,  $(CH_3(CH_2)_3)_4N)_7[PW_{11}O_{39}]$  (2), is shown in Figure 2.

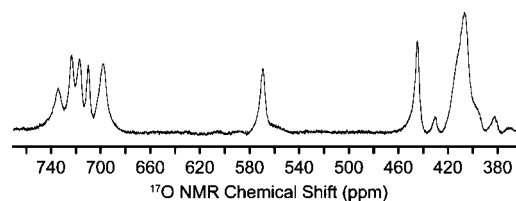


**Figure 2.**  $^{17}O$  NMR spectrum of an  $^{17}O$ -enriched sample of  $[PW_{11}O_{39}]^{7-}$  in 50/50 (vol %)  $CDCl_3/CH_3CN$ .

The spectrum shows  $W\equiv O$  peaks at 700–740 ppm,  $W-O-W$  peaks at 400–450 ppm, and a single isolated peak at 570 ppm, which is assigned to the terminal oxygen atoms in the vacant site of  $\{PW_{11}\}$  based on a comparison to the literature values for diamagnetic transition-metal-substituted derivatives of this POM.<sup>21</sup> To our knowledge, this is the first report of the  $^{17}O$  NMR spectrum of  $\{PW_{11}\}$  or any POM with oxygens containing such high local electron densities. During the counteranion exchange and  $^{17}O$  enrichment steps described in our 2007 publication,  $\{P_2W_{19}\}$  partially decomposed to  $\{PW_{11}\}$ , and the reported  $^{17}O$  NMR spectrum was actually that of  $\{PW_{11}\}$ .

That 2007 publication also incorrectly describes a second terminal Au-oxo complex, “ $K_7H_2[Au(O)(OH_2)P_2W_{20}O_{70}(OH_2)_2]$ ”.<sup>15</sup> This complex has a  $^{31}P$  NMR chemical shift distinct from all other polytungstates in this structural class, including  $[P_2W_{21}O_{71}(OH_2)_3]^{6-}$ ;<sup>22</sup> however, there is little information on POM  $^{31}P$  NMR chemical shifts as a function of the medium and in particular, pH. Thus, in this study we now undertake a careful evaluation of the pH dependences of these complexes. As we originally observed, a mixed sample of “ $K_7H_2[Au(O)(OH_2)P_2W_{20}O_{70}(OH_2)_2]$ ” and  $K_4H_2[P_2W_{21}O_{71}(OH_2)_3]$  gives two narrow peaks at –13.20 ppm and –13.27 ppm, respectively, strongly suggesting two distinct phosphorus-containing POMs given that proton exchange between POMs in aqueous solution is almost always in the fast exchange limit. We now report that when HCl is directly titrated into an NMR tube containing both of these complexes, the peak corresponding to “ $K_7H_2[Au(O)(OH_2)P_2W_{20}O_{70}(OH_2)_2]$ ” slowly shifts and finally merges with the peak corresponding to  $K_4H_2[P_2W_{21}O_{71}(OH_2)_3]$ , indicating that they are actually the same complex (Figure 3). Bini and Bagno have simulated  $^{17}O$  and  $^{183}W$  NMR spectra of some of these



compounds as part of a broader computational study on related noble metal complexes.<sup>16c</sup>

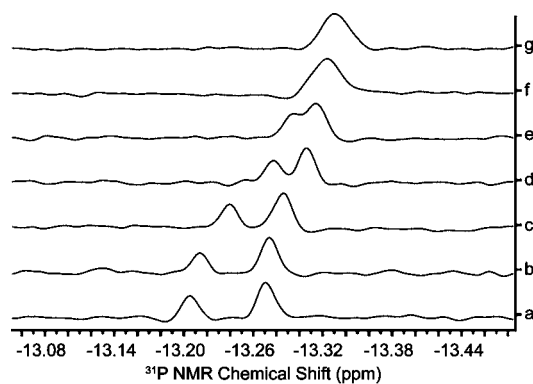
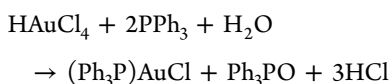


**Figure 3.** Acid titration of a mixture of “ $\text{K}_7\text{H}_2[\text{Au}(\text{O})(\text{OH}_2)\text{P}_2\text{W}_{20}\text{O}_{70}(\text{OH}_2)_2]$ ” and  $\text{K}_4\text{H}_2[\text{P}_2\text{W}_{21}\text{O}_{71}(\text{OH}_2)_3]$  in the same NMR tube followed by  $^{31}\text{P}$  NMR spectroscopy. Spectrum a: natural pH. Spectra b–g are acquired after the sequential addition of aliquots of  $30.0 \mu\text{L}$  of  $1.0 \text{ M}$  HCl and thorough mixing under identical data acquisition parameters.

We originally reported a reactivity study of oxo transfer from “ $\text{K}_7\text{H}_2[\text{Au}(\text{O})(\text{OH}_2)\text{P}_2\text{W}_{20}\text{O}_{70}(\text{OH}_2)_2]$ ” to triphenylphosphine which was followed by  $^{17}\text{O}$  and  $^{31}\text{P}$  NMR spectroscopy along with control experiments. In that study, we initially noted that “[a]ddition of triphenylphosphine to the *cis*-dicyclohexano-18-crown-6 salt of (the gold complex) in  $\text{CH}_3\text{CN}/\text{CDCl}_3$  under argon immediately yields a clear, colorless solution, and triphenylphosphine oxide ( $\text{Ph}_3\text{PO}$ , confirmed by  $^{31}\text{P}$  NMR spectroscopy).” These observations are now interpreted as the reaction between the Au(III) counter cations and triphenylphosphine, with a trace amount of water originating from nondried  $\text{CH}_3\text{CN}$  originally used as the NMR solvent:<sup>23</sup>



The previously observed color change from yellow to colorless and the resulting formation of  $(\text{Ph}_3\text{P})\text{AuCl}$  and  $\text{Ph}_3\text{PO}$  by  $^{31}\text{P}$  NMR spectroscopy are consistent with this assignment.

Thus, the original assignments were heavily, but not solely, based on X-ray and neutron crystallographic data. A historic example of misinterpretation of X-ray data is the “bond stretch isomer” phenomenon, which was originally supported by X-ray data and later explained with theory<sup>24</sup> but was finally shown to be the consequence of apparent bond lengthening resulting from compositional disorder.<sup>25</sup> This example is in contrast to the data presented here for three reasons: (i) this study identifies bond distance shortening, rather than lengthening, based on crystallographic libration; (ii) these complexes are pure polyanion complexes with noble metal counter cations, rather than subject to compositional disorder of the terminal ligand; (iii) our assignments were supported by an extensive number of additional experiments, while the “bond stretch isomers” were primarily based on X-ray data.

All of the information above indicates that the reported “Pt-oxo” and “Au-oxo” polyoxometalate complexes are in fact their isostructural W-oxo analogues with (disordered) noble metal counterions. However, investigation of the Pd-oxo complex reported in 2005 requires a different approach because a

different phenomenon is responsible for originally complicating its interpretation.

We incorrectly reported this first Pd-oxo complex as “ $\text{K}_{10}\text{Na}_3[\text{Pd}^{\text{IV}}(\text{O})(\text{OH})\text{WO}(\text{OH}_2)(\text{PW}_9\text{O}_{34})_2]$ .”<sup>14</sup> A new crystal structure refinement of this complex, **3**, is presented in Figure 4.

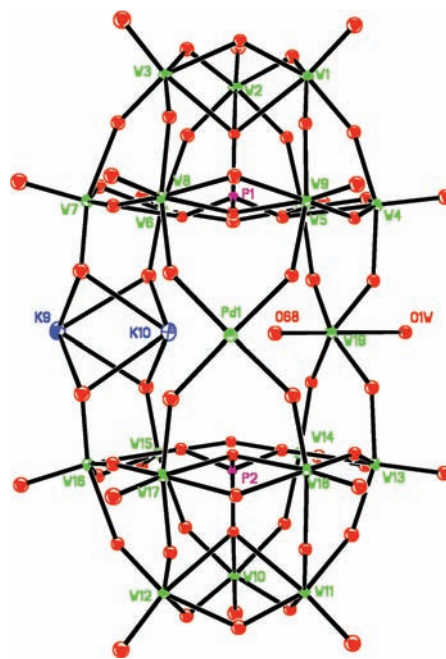


**Figure 4.** Thermal ellipsoid plot of  $[\text{PdWO}(\text{OH}_2)(\text{PW}_9\text{O}_{34})_2]^{12-}$  (50% probability surfaces). All atoms except oxygen are refined anisotropically.

The structure reveals two  $[\alpha\text{-PW}_9\text{O}_{34}]^{9-}$  units coordinated by two transition metal units: a Pd(II) ion in a conventional square planar environment and a  $[\text{O}\equiv\text{W}(\text{OH}_2)]^{4+}$  unit. The remaining position in the belt is a vacant site which is coordinated to two potassium atoms in the solid state. As noted previously, Pd1 is doming out of the plane defined by its four equatorial oxygen donors of the polytungstate by a distance of  $0.10 \text{ \AA}$ , but this distance is comparable to other reported Pd-containing POMs which have a Pd doming distance on average of  $0.06 \text{ \AA}$ .<sup>26</sup> There are two electron density peaks near Pd1 in the structure of **3** at the same positions and intensities as in the original report. We decided to drop these peaks in the final refinement of **3**, and the resulting structure refined satisfactorily without them. We therefore conclude that those peaks must result from the  $\text{K}^+$  ions and arise from a small amount of positional disorder between the Pd and the vacant site. We had previously refined these peaks as half-occupied terminal oxo and hydroxo ligands bound to the Pd, respectively. The previous oxo assignment of this complex was supported by  $^{17}\text{O}$  NMR, which showed a single, isolated peak at  $570 \text{ ppm}$  that we had assigned to an oxo bound to Pd based on the established correlation between chemical shift and oxygen  $\pi$ -bond order, the experimentally determined diamagnetic nature of the complex, and the absence of such a peak in all known polytungstate  $^{17}\text{O}$  NMR spectra. However, the previously published complex decomposes in solution to a palladium-containing Keggin-type species which is tentatively assigned  $[\text{Pd}^{\text{II}}\text{PW}_{11}\text{O}_{39}]^{5-}$  because of the cubic space group of the resulting crystals. Thus, the previously published peak at  $570$

ppm for the terminal oxo atom, consistent with arguments given regarding  $^{17}\text{O}$  NMR chemical shifts as a function of  $\pi$ -bonding to oxygen etc., belongs to the polytungstate oxygens coordinated to the Pd atom in the decomposition product. The new X-ray refinement and elemental analyses give rise to the formula  $\text{K}_{12}[\text{PdWO}(\text{OH}_2)(\text{PW}_9\text{O}_{34})_2]$  for **3**.

We also previously used Pd K-edge EXAFS data as a second independent structural method to confirm the short Pd=O bond distance in **3**. The multishell fits to the EXAFS spectra assumed an overall distorted octahedral Pd environment based on the crystallographic results. A model with the split first shell of one oxygen at  $1.68 \pm 0.03 \text{ \AA}$  and five oxygens at  $1.96 \pm 0.03 \text{ \AA}$  resulted in a significantly lower fit error than the models with a single shell of five or six oxygen atoms at  $\sim 1.96 \text{ \AA}$  (0.151 vs 0.217 or 0.263, respectively). A short-distance Pd=O component of  $1.68 \text{ \AA}$  was deemed to be important for a proper fit to the data within the framework. Now, assuming a square planar coordination, we obtain the fit error of 0.193 (Supporting Information, fit 6). Although this value is higher than that for the originally reported fit with the short Pd=O bond (Supporting Information, fit 4), the fit error difference is less significant, the metrical parameters unchanged, with the  $\sigma^2$  parameters absorbing the difference. The visual quality of fits 4 and 6 are also very close. Therefore, the currently proposed four-oxygen coordination of Pd would also be an acceptable model for the EXAFS data of **3**. Such uncertainty in the first-shell analysis arises from the exceptionally strong scattering from four tungsten atoms at  $3.6 \text{ \AA}$ , which dominates the spectrum and shortens the  $k$ -range available for analysis of the lighter atom contributions, with a longer  $k$ -range of the data being crucial for definitive resolution and evaluation of individual Pd=O contributions. This example highlights the difficulty in using EXAFS to provide definitive identification of coordination environments in certain situations, and considerable care should be exercised when using models based on X-ray diffraction data to provide independent support for the result of the X-ray diffraction study.

The original interpretation of electronic absorption spectra was conducted under the assumption that the X-ray and neutron diffraction data revealed the presence of late-transition-metal-oxo species. For example, the low-temperature (5 K) electronic spectrum of **3** possesses two weak ligand-field absorption bands in the visible region of the spectrum, at  $19\,750 \text{ cm}^{-1}$  (506 nm; band 1) and  $22\,700 \text{ cm}^{-1}$  (441 nm; band 2). The intense oxygen-to-tungsten charge transfer bands ( $E > 26\,000 \text{ cm}^{-1}$ ) found in polytungstates are observed at higher energy. Our original analysis was based on a Pd(IV)-oxo structure and yielded tentative assignments for bands 1 and 2 as arising from  $xz, yz \rightarrow x^2 - y^2$  and  $xy \rightarrow x^2 - y^2$  one-electron promotions. These data can also be interpreted in the context of a square planar Pd(II) ion. Using a simple angular overlap model,<sup>27</sup> band 1 can be assigned as an  $xy \rightarrow x^2 - y^2$  one-electron promotion ( $^1A_{1g} \rightarrow ^1A_{2g}$  in  $D_{4h}$ ) and band 2 as  $xz, yz \rightarrow x^2 - y^2$  ( $^1A_{1g} \rightarrow ^1E_g$  in  $D_{4h}$ ). A definitive assignment would require an analysis of polarized single crystal absorption data. The similar spectral assignments clearly indicate the reliance on structural data for detailed electronic structure information on these POM structures.

The oxidation state of palladium was previously assigned as +IV based on data from X-ray, low temperature UV–vis, cyclic voltammetry, and controlled potential coulometry studies. The new crystal structure of this complex reveals that it is actually Pd(II) in a conventional square planar environment with a

bond valence sum of 2.29.<sup>28</sup> Charge balance also mandates an oxidation state of +II for Pd based on the molecular formula,  $\text{K}_{12}[\text{PdWO}(\text{OH}_2)(\text{PW}_9\text{O}_{34})_2]$ , which is determined by elemental analysis on three different samples synthesized by three different researchers in our lab. These observations provide compelling evidence for a +II oxidation state for Pd; nevertheless, we provide herein an additional study. The original cyclic voltammetry and controlled potential coulometry studies included control experiments on  $\text{PdSO}_4$  and known Pd(II)-containing POMs and suggested a +IV oxidation state for Pd in **3**. However, deposition of  $\text{Pd}^0$  on the surface of the electrode complicates this interpretation. We have now conducted galloctyanin colorimetric redox titrations.<sup>29</sup> In buffered solutions, one equivalent of **3** was added to three equivalents of galloctyanin, and the absorbance value at 626 nm corresponding to galloctyanin was monitored with time. The data were fit to an exponential reaction rate law and compared to that of its reaction with  $\text{K}_8[\text{Pd}^{\text{IV}}\text{P}_2\text{W}_{20}\text{O}_{70}]$ , which displayed nearly identical behavior (see Supporting Information for the resulting kinetic plot). This strongly suggests that Pd is the same oxidation state in **3** and in  $\text{K}_8[\text{Pd}^{\text{IV}}\text{P}_2\text{W}_{20}\text{O}_{70}]$ . If the oxidation state in **3** were +IV, then the rate of reaction and the final absorbance value for **3** would be twice that of  $\text{K}_8[\text{Pd}^{\text{IV}}\text{P}_2\text{W}_{20}\text{O}_{70}]$ .

## EXPERIMENTAL METHODS

**General Methods and Materials.** The complexes  $\text{K}_{14}[\text{P}_2\text{W}_{19}\text{O}_{69}(\text{OH}_2)] \cdot 2.4\text{H}_2\text{O}$ ,<sup>18</sup>  $\text{K}_7[\text{PW}_{11}\text{O}_{39}] \cdot 1.4\text{H}_2\text{O}$ ,<sup>30</sup>  $\text{K}_4\text{H}_2[\text{P}_2\text{W}_{21}\text{O}_{71}(\text{OH}_2)_3] \cdot 2.8\text{H}_2\text{O}$ ,<sup>22</sup> and the originally formulated complexes “ $\text{K}_7\text{Na}_9[\text{Pt}^{\text{IV}}(\text{O})(\text{H}_2\text{O})(\text{PW}_9\text{O}_{34})_2]$ ”,<sup>13</sup> “ $\text{K}_{10}\text{Na}_3[\text{Pd}^{\text{IV}}(\text{O})(\text{OH})\text{WO}(\text{OH}_2)(\text{PW}_9\text{O}_{34})_2]$ ”,<sup>14</sup> “ $\text{K}_{15}\text{H}_2[\text{Au}(\text{O})(\text{OH}_2)\text{P}_2\text{W}_{18}\text{O}_{68}]$ ”,<sup>15</sup> and “ $\text{K}_7\text{H}_2[\text{Au}(\text{O})(\text{OH}_2)\text{P}_2\text{W}_{20}\text{O}_{70}(\text{OH}_2)_2]$ ”<sup>15</sup> were synthesized according to published procedures and checked by  $^{31}\text{P}$  NMR spectroscopy and FT-IR spectroscopy.  $\text{Na}_2\text{WO}_4$  (95%),  $\text{PdSO}_4 \cdot 2\text{H}_2\text{O}$  (99%), and  $[\text{CH}_3(\text{CH}_2)_3]_4\text{NCl}$  (99.9%) were purchased from Alfa Aesar. Galloctyanin (7-dimethylamino-4-hydroxy-3-oxo-phenoxazine-1-carboxylic acid) was purchased from Aldrich.  $\text{H}_3\text{BO}_3$  and  $\text{Na}_2\text{B}_4\text{O}_7 \cdot 10\text{H}_2\text{O}$  were purchased from Fischer Scientific. All chemicals were used as received. Infrared spectra (KBr pellets) were recorded on a Thermo Nicolet 6700 instrument. Electronic absorption spectra were acquired using an Agilent 8453 spectrophotometer equipped with a diode-array detector and a temperature controller (Agilent 89090A).

**X-Ray Crystallography.** *a. Instrumentation and Methods.* The complete data sets for complexes **1** and **3** were collected at Emory University (see Table 2 for X-ray refinement details). Single crystals suitable for X-ray analysis were each coated with Paratone-N oil, suspended in a small fiber loop, and placed in a cooled gas stream on a Bruker D8 SMART APEX CCD sealed tube diffractometer. Diffraction intensities were measured using graphite monochromated Mo  $K\alpha$  radiation ( $\lambda = 0.71073 \text{ \AA}$ ) at 173(2) K and a combination of  $\varphi$  and  $\omega$  scans with 10 s frames traversing about  $\omega$  at  $0.5^\circ$  increments. Data collection, indexing, and initial cell refinements were carried out using SMART;<sup>31</sup> frame integration and final cell refinements were done using SAINT.<sup>32</sup> The molecular structure of each complex was determined using direct methods and Fourier techniques and refined by full-matrix least-squares. A multiple absorption correction, including face index, for each data set at 173(2) K was applied using the program SADABS.<sup>33</sup>

*b. Refinement Details.* The structures of **1** and **3** were solved using direct methods and difference Fourier techniques. All of the heavy atoms were refined anisotropically. Some of the potassium ions and solvent water molecules were refined with partial occupancies; not all of the counter cations and solvent water molecules could be located in difference Fourier maps because of disorder. Scattering factors and anomalous dispersion corrections are taken from the International Tables for X-ray Crystallography. Structure solution, refinement,

Table 2. X-Ray Refinement Details of 1 and 3

complex	1	3
molecular formula	K <sub>14</sub> O <sub>84</sub> H <sub>30</sub> P <sub>2</sub> W <sub>19</sub>	K <sub>12</sub> O <sub>86.50</sub> H <sub>35</sub> P <sub>2</sub> PdW <sub>19</sub>
fw (g mol <sup>-1</sup> )	5476.47	5549.76
temp (K)	173(2)	173(2)
radiation (λ, Å)	0.71073	0.71073
cryst syst	orthorhombic	triclinic
space group	<i>Fddd</i>	<i>P</i> $\bar{1}$
<i>a</i> (Å)	28.645(9)	11.984(2)
<i>b</i> (Å)	31.827(11)	17.335(4)
<i>c</i> (Å)	38.707(13)	23.029(5)
α (deg)	90	90.382(3)
β (deg)	90	103.293(3)
γ (deg)	90	108.724(3)
volume (Å <sup>3</sup> )	35290(20)	4392.7(15)
<i>Z</i>	16	2
ρ <sub>calcd</sub> (g cm <sup>-3</sup> )	3.983	4.169
μ (mm <sup>-1</sup> )	25.274	25.679
<i>F</i> (000)	36768	4804
cryst size (mm <sup>3</sup> )	0.29 × 0.21 × 0.20	0.46 × 0.19 × 0.18
θ range	1.09–29.13	1.82–28.28
reflns collected	158284	76467
independent reflns	11898 [R(int) = 0.0933]	21689 [R(int) = 0.0720]
max./min transmission	0.0810 and 0.0512	0.0931 and 0.0300
refinement method	full-matrix least-squares on <i>F</i> <sup>2</sup>	full-matrix least-squares on <i>F</i> <sup>2</sup>
data/restraints/param.	11898/0/335	21689/0/664
goodness-of-fit on <i>F</i> <sup>2</sup>	1.082	1.013
final <i>R</i> indices [R > 2σ (I)]	<i>R</i> <sub>1</sub> <sup>a</sup> = 0.0497, <i>wR</i> <sub>2</sub> <sup>b</sup> = 0.1844	<i>R</i> <sub>1</sub> <sup>a</sup> = 0.0547, <i>wR</i> <sub>2</sub> <sup>b</sup> = 0.1595
<i>R</i> indices (all data)	<i>R</i> <sub>1</sub> <sup>a</sup> = 0.0675, <i>wR</i> <sub>2</sub> <sup>b</sup> = 0.2129	<i>R</i> <sub>1</sub> <sup>a</sup> = 0.0759, <i>wR</i> <sub>2</sub> <sup>b</sup> = 0.1754
largest diff. peak and hole (e Å <sup>-3</sup> )	7.265 and -5.263	16.846 and -3.783

<sup>a</sup>*R*<sub>1</sub> = ∑||*F*<sub>o</sub>|| - ||*F*<sub>c</sub>||/∑||*F*<sub>o</sub>||. <sup>b</sup>*wR*<sub>2</sub> = {∑[*w*(*F*<sub>o</sub><sup>2</sup> - *F*<sub>c</sub><sup>2</sup>)<sup>2</sup>]/∑[*w*(*F*<sub>o</sub><sup>2</sup>)<sup>2</sup>]}<sup>0.5</sup>.

graphics, and generation of publication materials were performed by using SHELXTL, V6.14.<sup>34</sup>

**NMR Spectroscopy.** The <sup>31</sup>P NMR spectra (162.13 MHz) were acquired on a Varian INOVA 400 spectrometer. The spectrometer was locked on the <sup>2</sup>H resonance of D<sub>2</sub>O, and all chemical shifts were reported relative to an external standard H<sub>3</sub>PO<sub>4</sub> (0 ppm). The <sup>17</sup>O NMR spectra (81.32 MHz) were acquired on a Varian UNITY 600 spectrometer. The spectrometer was locked on the <sup>2</sup>H resonance of CDCl<sub>3</sub>, and all chemical shifts were reported relative to <sup>2</sup>H<sub>2</sub><sup>17</sup>O (0 ppm). Spectral parameters for <sup>17</sup>O NMR were the following: pulse width, 10 μs; sweep width, 80 000 Hz; 0.01 s delay; 20 088 transients; 31 998 data points. Spectra were obtained using cylindrical 5-mm-o.d. sample tubes (7 in). Data were processed using Mnova (<sup>31</sup>P) and ACD (<sup>17</sup>O).

**Methods for <sup>31</sup>P NMR Titration.** Samples of “K<sub>7</sub>H<sub>2</sub>[Au(O)(OH<sub>2</sub>)<sub>2</sub>]<sub>2</sub>” (0.020 g, 3.49 × 10<sup>-6</sup> mol) and K<sub>4</sub>H<sub>2</sub>[P<sub>2</sub>W<sub>21</sub>O<sub>71</sub>(OH<sub>2</sub>)<sub>3</sub>] (0.020 g, 3.46 × 10<sup>-6</sup> mol) were dissolved together in 0.70 mL of D<sub>2</sub>O, and the <sup>31</sup>P NMR spectrum was acquired immediately (spectrum a). Separate control experiments show that the peak at -13.20 ppm corresponds to “K<sub>7</sub>H<sub>2</sub>[Au(O)(OH<sub>2</sub>)<sub>2</sub>]<sub>2</sub>” and the peak at -13.27 ppm corresponds to K<sub>4</sub>H<sub>2</sub>[P<sub>2</sub>W<sub>21</sub>O<sub>71</sub>(OH<sub>2</sub>)<sub>3</sub>]. In addition, these two NMR peaks are unchanged for days together or separate in solution and do not undergo any broadening or exchange. Immediately after the first spectrum was acquired, 30.0 μL of 1.0 M HCl was added to the NMR tube and the solution thoroughly mixed, and spectrum b was acquired within 2 min. This process was repeated for the rest of the spectra.

**Synthetic Procedure for (CH<sub>3</sub>(CH<sub>2</sub>)<sub>3</sub>)<sub>4</sub>N<sub>7</sub>[PW<sub>11</sub>O<sub>39</sub>] (2).** A 0.20 g (0.061 mmol) sample of {PW<sub>11</sub>} was dissolved in 1.0 mL water, and

then a 10.0 mL solution of [CH<sub>3</sub>(CH<sub>2</sub>)<sub>3</sub>]<sub>4</sub>NCl (0.169 g, 0.608 mmol) in CH<sub>2</sub>Cl<sub>2</sub> was added quickly under vigorous stirring at room temperature. Upon standing, the mixture separated into a clear organic layer and a cloudy white aqueous later. The organic layer was separated and filtered on a 0.45 μm nylon membrane filter and then was concentrated to dryness at room temperature on a rotary evaporator. The resulting solids were dissolved in 0.5 mL of CH<sub>3</sub>CN, and a 0.10 mL sample of 10% <sup>17</sup>O-enriched water was added to this CH<sub>3</sub>CN solution. The mixture was kept for 2 days at 50 °C in a capped NMR tube. This process incorporates <sup>17</sup>O into the polyanion structure. The mixture was then concentrated using a rotary evaporator at room temperature, and the resulting solids were redissolved in 0.5 mL of 50/50 CH<sub>3</sub>CN/CDCl<sub>3</sub>. Note, this is the same <sup>17</sup>O enrichment procedure as described for “K<sub>15</sub>H<sub>2</sub>[Au(O)(OH<sub>2</sub>)<sub>2</sub>]<sub>2</sub>” and gives the same <sup>31</sup>P NMR spectrum: a single peak at -15.1 ppm in CH<sub>3</sub>CN/CDCl<sub>3</sub> solvent.

**Chemical Reduction of 3.** A sample of 3 (0.011 g, 2.0 × 10<sup>-6</sup> mol) and a sample of K<sub>8</sub>[Pd<sup>II</sup>P<sub>2</sub>W<sub>20</sub>O<sub>70</sub>] (0.011 g, 1.99 × 10<sup>-6</sup> mol) were each dissolved in separate 2.50 mL portions of sodium borate buffer solution (40 mM, pH 9.0). A sample of gallocyanin (0.001 g, 2.97 × 10<sup>-6</sup> mol) was dissolved in 125 mL of a borate buffer. A 1.00 mL sample of gallocyanin solution was placed in a 0.5 cm quartz cuvette, and the UV-vis spectrum was recorded. A 10 μL aliquot of the solution of 3 (8.0 × 10<sup>-9</sup> mol, 0.33 equiv) was then added, and the resulting spectra were recorded over a period of 2 h at 25 °C. The same procedure was followed for the solution of K<sub>8</sub>[Pd<sup>II</sup>P<sub>2</sub>W<sub>20</sub>O<sub>70</sub>].

## CONCLUSIONS

In summary, new X-ray, <sup>17</sup>O NMR, <sup>31</sup>P NMR, and other data presented herein allow us to confidently reinterpret our original models. These results are completely consistent with the Oxo Wall, in contrast to what we previously claimed. These complexes were originally assigned quite defensibly based on the extensive characterization conducted at the time, but our new data indicate that the previously reported “Pt-oxo” and “Au-oxo” complexes are in fact the tungsten analogues of these complexes that cocrystallize with noble metal counter cations. The previously reported “Pd-oxo” complex suffered from multiple crystallographic disorder issues that we initially interpreted incorrectly as oxo atoms in the original X-ray structure refinement. We have identified here the decomposition pathway of these species in solution which previously led to the assignment of oxo atoms in the original <sup>17</sup>O NMR spectra as well as, identified here, the pH dependence of the <sup>31</sup>P NMR signal of [P<sub>2</sub>W<sub>21</sub>O<sub>71</sub>(OH<sub>2</sub>)<sub>3</sub>]<sup>6-</sup>. Therefore, the problem of interpretation arose chiefly for four reasons: (i) We originally did not collect and compare the X-ray structure of {P<sub>2</sub>W<sub>19</sub>} at 173 K, now presented here, to our previously reported complexes at the same temperature. (ii) The neutron diffraction data originally indicated to us that it was Pt (or Au) and *not* W in the central bridging position. (iii) The pertinent <sup>17</sup>O and <sup>31</sup>P NMR data, now presented here, were not available for comparison at the time of our original publications. (iv) We originally did not recognize the unusual crystallographic disorder of the Pd-substituted POM. This study highlights the critical interplay between crystallography, neutron diffraction, EXAFS, and spectroscopy in determining the structure of large molecules that may be subject to rare types of crystallographic disorder. We urge caution for the application of these techniques for compounds that possess uncommon and complex geometrical structures.



## ASSOCIATED CONTENT

### Supporting Information

Crystallographic information files (CIF) of **1** and **3**, complete list of experimental techniques used to characterize the late-transition-metal-oxo complexes, details of the neutron diffraction and EXAFS studies, and kinetic plot of gallocyanin oxidation. This material is available free of charge via the Internet at <http://pubs.acs.org>.

## AUTHOR INFORMATION

### Corresponding Author

\*E-mail: [chill@emory.edu](mailto:chill@emory.edu).

### Present Address

<sup>○</sup>Institute of Inorganic Chemistry, RWTH Aachen University, 52074 Aachen, Germany.

### Notes

The authors declare no competing financial interest.

## ACKNOWLEDGMENTS

We thank the National Science Foundation (grant CHE-0911610) for support of this research. We also thank Dr. Ulrich Kortz of Jacobs University (Bremen, Germany) for challenging our work.

## REFERENCES

- (1) (a) Nugent, W. A.; Mayer, J. M. *Metal-Ligand Multiple Bonds*; John Wiley & Sons, Inc.: New York, 1988. (b) Holm, R. H.; Donahue, J. P. *Polyhedron* **1993**, *12*, 571. (c) Parkin, G. *Prog. Inorg. Chem.* **1998**, *47*, 1. (d) Rogal, J.; Reuter, K.; Scheffler, M. *Phys. Rev. B: Condens. Matter.* **2007**, *75* (20), 205433.
- (2) (a) Ballhausen, C. J.; Gray, H. B. *Inorg. Chem.* **1962**, *1*, 111. (b) Gray, H. B.; Hare, C. R. *Inorg. Chem.* **1962**, *1*, 363.
- (3) (a) Sunil, K. K.; Harrison, J. F.; Rogers, M. T. *J. Chem. Phys.* **1982**, *76*, 3087. (b) Garner, C. D.; Kendrick, J.; Lambert, P.; Mabbs, F. E.; Hillier, I. H. *Inorg. Chem.* **1976**, *15*, 1287. (c) Azuma, N.; Ozawa, T.; Tsuboyama, S. *J. Chem. Soc., Dalton Trans.* **1994**, 2609.
- (4) (a) Mayer, J. M.; Thorn, D. L.; Tulip, T. H. *J. Am. Chem. Soc.* **1985**, *107*, 7454. (b) Spaltenstein, E.; Erikson, T. K. G.; Critchlow, S. C.; Mayer, J. M. *J. Am. Chem. Soc.* **1989**, *111*, 617.
- (5) Holm, R. H. *Chem. Rev.* **1987**, *87*, 1401.
- (6) (a) Winkler, J. R.; Gray, H. B. *Struct. Bonding (Berlin)* **2011**, *142*, 17–28. (b) Gray, H. B.; Winkler, J. R. Abstracts of Papers, 237th ACS National Meeting, Salt Lake City, UT, United States, March 22–26, 2009. (c) Abstracts of Papers, 236th ACS National Meeting, Philadelphia, PA, United States, August 17–21, 2008.
- (7) (a) Mayer, J. M. *Comments Inorg. Chem.* **1988**, *8*, 125. (b) Betley, T. A.; Wu, Q.; Voorhis, T. V.; Nocera, D. G. *Inorg. Chem.* **2008**, *47*, 1849.
- (8) MacBeth, C. E.; Golombek, A. P.; Young, V. G., Jr.; Yang, C.; Kuczera, K.; Hendrich, M. P.; Borovik, A. S. *Science* **2000**, *289*, 938.
- (9) Hay-Motherwell, R. S.; Wilkinson, G.; Hussain-Bates, B.; Hursthouse, M. B. *Polyhedron* **1993**, *12* (16), 2009.
- (10) Poverenov, E.; Efremenko, I.; Frenkel, A. I.; Ben-David, Y.; Shimon, L. J. W.; Leitus, G.; Konstantinovski, L.; Martin, J. M. L.; Milstein, D. *Nature* **2008**, *455*, 1093.
- (11) Putaj, P.; Lefebvre, F. *Coord. Chem. Rev.* **2011**, *255*, 1642.
- (12) Rong, C.; Pope, M. T. *J. Am. Chem. Soc.* **1992**, *114*, 2932.
- (13) Anderson, T. M.; Neiwert, W. A.; Kirk, M. L.; Piccoli, P. M. B.; Schultz, A. J.; Koetzle, T. F.; Musaev, D. G.; Morokuma, K.; Cao, R.; Hill, C. L. *Science* **2004**, *306*, 2074.
- (14) Anderson, T. M.; Cao, R.; Slonkina, E.; Hedman, B.; Hodgson, K. O.; Hardcastle, K. I.; Neiwert, W. A.; Wu, S.; Kirk, M. L.; Knottenbelt, S.; Depperman, E. C.; Keita, B.; Nadjo, L.; Musaev, D. G.; Morokuma, K.; Hill, C. L. *J. Am. Chem. Soc.* **2005**, *127*, 11948.
- (15) Cao, R.; Anderson, T. M.; Piccoli, P. M. B.; Schultz, A. J.; Koetzle, T. F.; Geletii, Y. V.; Slonkina, E.; Hedman, B.; Hodgson, K. O.; Hardcastle, K. I.; Fang, X.; Kirk, M. L.; Knottenbelt, S.; Kögerler, P.; Musaev, D. G.; Morokuma, K.; Takahashi, M.; Hill, C. L. *J. Am. Chem. Soc.* **2007**, *129*, 11118.
- (16) (a) Cao, R.; Anderson, T. M.; Hillesheim, D. A.; Kögerler, P.; Hardcastle, K. I.; Hill, C. L. *Angew. Chem., Int. Ed.* **2008**, *47*, 9380. (b) Kortz, U.; Lee, U.; Joo, H.-C.; Park, K.-M.; Mal, S. S.; Dickman, M. H.; Jameson, G. B. *Angew. Chem., Int. Ed.* **2008**, *47*, 9383. (c) Bagno, A.; Bini, R. *Angew. Chem., Int. Ed.* **2010**, *49*, 1083. (d) Limberg, C. *Angew. Chem., Int. Ed.* **2009**, *48*, 2270. (e) Ritter, S. K. *Chem. Eng. News* **2007**, *85* (38), 35. (f) Lee, U.; Joo, H.-C.; Park, K.-M.; Ozeki, T. *Acta Crystallogr.* **2003**, *c59*, m152.
- (17) Note: in ref 16a, we provided five experimental lines of evidence that the compound formulated by Uk Lee and co-workers as  $(\text{CH}_6\text{N}_3)_8[\alpha\text{-SiPt}_2\text{W}_{10}\text{O}_{40}]$  in ref 16f was actually  $(\text{CH}_6\text{N}_3)_8[\alpha\text{-SiW}_{11}\text{O}_{39}]$ . One of the criteria distinguishing this system from our putative  $\text{K}_7\text{Na}_9[\text{Pt}^{\text{IV}}(\text{O})(\text{H}_2\text{O})(\text{PW}_9\text{O}_{34})_2]$  was the more intense Pt-based optical transitions of our complex. We now have to conclude that the intensities of these transitions are of limited use in assigning the Pt oxidation state in POM systems.
- (18) Tourné, C. M.; Tourné, G. F. *J. Chem. Soc., Dalton Trans.* **1988**, 2411.
- (19) (a) Schomaker, V.; Trueblood, K. N. *Acta Crystallogr.* **1968**, *B24*, 63. (b) Busing, W. R.; Levy, H. A. *Acta Crystallogr.* **1964**, *17*, 142.
- (20) (a) Filowitz, M.; Klemperer, W. G.; Messerle, L.; Shum, W. J. *Am. Chem. Soc.* **1976**, *98*, 2345–2346. (b) Filowitz, M.; Ho, R. K. C.; Klemperer, W. G.; Shum, W. *Inorg. Chem.* **1979**, *18*, 93–103. (c) Maksimovskaya, R. I.; Fedotov, M. A. *Zh. Strukt. Khim.* **1981**, *22*, 160–162. (d) Kintzinger, J. *NMR: Basic Princ. Prog.* **1981**, *17*, 1–64. (e) *<sup>17</sup>O NMR Spectroscopy in Organic Chemistry*; Boykin, D. W., Ed.; CRC Press, Inc.: Boca Raton, FL, 1991. (f) Kazansky, L. P.; Chaquin, P.; Fournier, M.; Hervé, G. *Polyhedron* **1998**, *17*, 4353–4364.
- (21) Detushcheva, L. G.; Fedotov, M. A.; Kuznetsova, L. I.; Vlasov, A. A.; Likhobolov, V. A. G. K. *Russ. Chem. Bull.* **1997**, *46*, 874.
- (22) Tourné, C. M.; Tourné, G. F.; Weakley, T. J. R. *J. Chem. Soc., Dalton Trans.* **1986**, 2237.
- (23) Braunstein, P.; Lehner, H.; Matt, D.; Burgess, K.; Ohlmeyer, M. *J. Inorg. Synth.* **1990**, *27*, 218.
- (24) (a) Chatt, J.; Manojlovic-Muir, L.; Muir, K. W. *J. Chem. Soc. D* **1971**, 655–656. (b) Jean, Y.; Lledos, A.; Burdett, J. K.; Hoffmann, R. J. *Am. Chem. Soc.* **1988**, *110*, 4506.
- (25) Yoon, K.; Parkin, G.; Rheingold, A. L. *J. Am. Chem. Soc.* **1992**, *114*, 2210.
- (26) (a) Bi, L.-H.; Kortz, U.; Keita, B.; Nadjo, L.; Borrmann, H. *Inorg. Chem.* **2004**, *43*, 8367. (b) Bi, L.-H.; Reicke, M.; Kortz, U.; Keita, B.; Nadjo, L.; Clark, R. J. *Inorg. Chem.* **2004**, *43*, 3915.
- (27) (a) Schönherr, T.; Atanasov, M. *Comprehensive Coordination Chemistry II*; Lever, A. B. P., Ed.; Elsevier: Amsterdam, 2004; Vol. 2, pp 113–141. (b) Adamsky, H.; Schönherr, T.; Atanasov, M. *Comprehensive Coordination Chemistry II*; Lever, A. B. P., Ed.; Elsevier: Amsterdam, 2004; Vol. 2, pp 661–664. (c) Adamsky, H. "AOMX." 1996. <http://www.aomx.des> (Accessed May 30, 2012).
- (28) Bond valence sum is a common method to quantify the oxidation state through crystallographic bond distances. See: Brown, I. D. *Chem. Rev.* **2009**, *109*, 6858–6919. The bond valence of Pd in the original publication of this complex was not reported due to lack of examples of Pd(IV) for comparison.
- (29) Balavoine, G. A.; Geletii, Y. V. *Nitric Oxide: Biol. Chem.* **1999**, *3* (1), 40.
- (30) Contant, R. *Can. J. Chem.* **1987**, *65*, 568–573.
- (31) Bruker APEX2; Bruker AXS Inc.: Madison, WI, 2007.
- (32) Bruker SAINT; Bruker AXS Inc.: Madison, WI, 2007.
- (33) Sheldrick, G. SADABS, 2.10 edition; Bruker AXS Inc.: Madison, WI, 2003.
- (34) Sheldrick, G. M. *Acta Crystallogr., Sect. A* **2008**, *64*, 112–122.